ORGANOMETALLICS
Article

Organometallics **2009,** *28,* 6003–6013 6003
DOI: 10.1021/om900490b

Investigating the Nature of the Active Species in Bis(imino)pyridine Cobalt Ethylene Polymerization Catalysts

Igor E. Soshnikov,[†,‡] Nina V. Semikolenova,[†] Alexey N. Bushmelev,[†,‡]
Konstantin P. Bryliakov,[†,‡] Oleg Y. Lyakin,[†,‡] Carl Redshaw,[§] Vladimir A. Zakharov,[†] and
Evgenii P. Talsi*[,†,‡]

[†] *Boreskov Institute of Catalysis, Siberian Branch of the Russian Academy of Sciences, 630090, Novosibirsk, Russian Federation,* [‡] *Novosibirsk State University, 630090, Novosibirsk, Russian Federation, and* [§] *School of Chemistry, University of East Anglia, Norwich NR4 7TJ, U.K.*

Received June 10, 2009

The activation of bis(imino)pyridine cobalt-based catalysts of ethylene polymerization with methylalumoxane (MAO), $AlMe_3$, and $AlMe_3/[CPh_3][B(C_6F_5)_4]$ has been studied by ^1H, ^2H, and ^{19}F NMR and EPR spectroscopy. The nature of the active sites of polymerization is discussed. The polymerization kinetics and the polymer properties for the different catalyst/activator systems were correlated with spectroscopic data.

Introduction

In the past decade, there has been much interest in iron and cobalt ethylene polymerization catalysts $LM^{II}Cl_2$/MAO and $LM^{II}Cl_2/AlR_3$, where M = Fe or Co, L = bis(imino)pyridine ligand, and R = alkyl.[1−38] NMR spectroscopic investigations define the structures of iron species formed in the $LFe^{II}Cl_2$/MAO and $LFe^{II}Cl_2/AlMe_3$ systems.[10,17,38] It was shown that ion pairs $[LFe^{II}(\mu\text{-Me})_2AlMe_2]^+[\text{Me-MAO}]^-$ predominate

---

*Corresponding author. Fax: +7 383 3308056. E-mail: talsi@catalysis.ru.

(1) Small, B. L.; Brookhart, M. *J. Am. Chem. Soc.* **1998**, *120*, 7143–7144.
(2) Small, B. L.; Brookhart, M.; Bennett, A. M. A. *J. Am. Chem. Soc.* **1998**, *120*, 4049–4050.
(3) Bennett, A. M. A. (Dupont) WO 98/27124, 1998; *Chem. Abstr.* **1998**, *129*, 122973x.
(4) Britovsek, G. J. P.; Gibson, V. C.; Kimberley, B. S.; Maddox, P. J.; McTavish, S. J.; Solan, G. A.; White, A. J. P.; Williams, D. J. *Chem. Commun.* **1998**, 849–850.
(5) Bennett, A. M. A. *CHEMTECH* **1999** (July), 24−28.
(6) Britovsek, G. J. P.; Bruce, M.; Gibson, V. C.; Kimberley, B. S.; Maddox, P. J.; Mastroianni, S.; McTavish, S. J.; Redshaw, C.; Solan, G. A.; Stromberg, S.; White, A. J. P.; Williams, D. J. *J. Am. Chem. Soc.* **1999**, *121*, 8728–8740.
(7) Britovsek, G. J. P.; Mastroianni, S.; Solan, G. A.; Baugh, S. P. D.; Redshaw, C.; Gibson, V. C.; White, A. J. P.; Williams, D. J.; Elsegood, M. R. J. *Chem.—Eur. J.* **2000**, *6*, 2221–2231.
(8) Ma, Z.; Qui, J.; Xu, D.; Hu, Y. *Macromol. Rapid Commun.* **2001**, *22*, 1280–1283.
(9) Britovsek, G. J. P.; Gibson, V. C.; Kimberley, B. S.; Mastroianni, S.; Redshaw, C.; Solan, G. A.; White, A. J. P. *J. Chem. Soc., Dalton Trans.* **2001**, 1639–1644.
(10) Talsi, E. P.; Babushkin, D. E.; Semikolenova, N. V.; Zakharov, V. A. *Macromol. Chem. Phys.* **2001**, *202*, 2046–2051.
(11) Kooistra, T. M.; Knujenburg, Q.; Smits, J. M. M.; D. Horton, A.; Budzelaar, P. H. M.; Gal, A. W. *Angew. Chem., Int. Ed.* **2001**, *40*, 4719–4722.
(12) Gibson, V. C.; Humphries, M. J.; Tellmann, K. P.; Wass, D. F.; White, A. J. P.; Williams, D. J. *Chem. Commun.* **2001**, 2252–2253.
(13) Abu-Surrah, A. S.; Lappalainen, K.; Piironen, P.; Lehmus, P.; Repo, T.; Leskela, M. *J. Organomet. Chem.* **2002**, *648*, 55–65.
(14) Semikolenova, N. V.; Zakharov, V. A.; Talsi, E. P.; Babushkin, D. E.; Sobolev, A. P.; Echevskaja, L. G.; Khysniyarov, M. M. *J. Mol. Catal. A* **2002**, *182*−*183*, 283–294.
(15) Chen, Y.; Qian, C.; Sun, J. *Organometallics* **2003**, *22*, 1231–1236.
(16) Paulino, I. S.; Schuchardt, U. *J. Mol. Catal. A* **2004**, *211*, 55–58.
(17) Bryliakov, K. P.; Semikolenova, N. V.; Zakharov, V. A.; Talsi, E. P. *Organometallics* **2004**, *23*, 5375–5378.
(18) Zhang, Z.; Chen, S.; Zhang, X.; Li, H.; Ke, Y.; Lu, Y.; Hu, Y. *J. Mol. Catal. A* **2005**, *230*, 1–8.
(19) Liu, J.-Y.; Zheng, Y.; Li, Y.-G.; Pan, L.; Li, Y.-S.; Hu, N.-H. *J. Organomet. Chem.* **2005**, *690*, 1233–1239.
(20) Tellmann, K. P.; Gibson, V. C.; White, A. J. P.; Williams, D. J. *Organometallics* **2005**, *24*, 280–286.
(21) Humphries, M. J.; Tellmann; Gibson, V. C.; White, A. J. P.; Williams, D. J. *Organometallics* **2005**, *24*, 2039–2050.
(22) Bouwkamp, M. W.; Bart, S. C.; Hawrelak, E. J.; Trovitch, R. J.; Lobkovsky, E.; Chirik, P. J. *Chem. Commun.* **2005**, 3406–3408.
(23) Barabanov, A. A.; Zakharov, V. A.; Semikolenova, N. V.; Echevskaja, L. G.; Matsko, M. A. *Macromol. Chem. Phys.* **2005**, *206*, 2292–2298.
(24) Scott, J.; Gambarotta, S.; Korobkov, I.; Knijnenburg, Q.; de Bruin, B.; Budzelaar, P. H. M. *J. Am. Chem. Soc.* **2005**, *127*, 17204–17206.
(25) Ionkin, A. S.; Marshall, W. J.; Adelman, D. J.; Fones, B. B.; Fish, B. M.; Schiffhauer, M. F. *Organometallics* **2006**, *25*, 2978–2992.
(26) Gibson, V. C.; Long, N. J.; Oxford, P. J.; White, A. J. P.; Williams, D. J. *Organometallics* **2006**, *25*, 1932–1939.
(27) Bart, S. C.; Chlopek, K.; Bill, E.; Bouwkamp, M. W.; Lobkovsky, E.; Neese, F.; Wieghardt, K.; Chirik, P. J. *J. Am. Chem. Soc.* **2006**, *128*, 13901–13912.
(28) Barabanov, A. A.; Bukatov, G. D.; Zakharov, V. A.; Semikolenova, N. V.; Mikenas, T. B.; Echevskaja, L. G.; Matsko, M. A. *Macromol. Chem. Phys.* **2006**, *207*, 1368–1375.
(29) Kissin, Y. V.; Qian, C.; Xie, G.; Chen, Y. *J. Polym. Sci., Part A: Polym. Chem.* **2006**, *44*, 6159–6170.
(30) Redshaw, C.; Gibson, V. C.; Solan, G. A. *Chem. Rev.* **2007**, *107*, 1745–1776.
(31) Bart, S. C.; Lobkovsky, E.; Bill, E.; Wieghardt, K.; Chirik, P. J. *Inorg. Chem.* **2007**, *46*, 7055–7063.
(32) Sun, W. H.; Zhang, S.; Zuo, W. *C. R. Chim.* **2008**, *11*, 307–316.
(33) Hanton, M. J.; Tenza, K. *Organometallics* **2008**, *27*, 5712–5716.
(34) Ionkin, A. S.; Marshall, W. J.; Adelman, D. J.; Fones, B. B.; Fish, B. M.; Schiffhauer, M. F. *Organometallics* **2008**, *27*, 1147–1156.
(35) Trovitch, R. J.; Lobkovsky, E.; Bill, E.; Chirik, P. J. *Organometallics* **2008**, *27*, 1470–1478.
(36) Fernández, I.; Trovitch, R. J.; Lobkovsky, E.; Chirik, P. J. *Organometallics* **2008**, *27*, 109–118.
(37) Barabanov, A. A.; Bukatov, G. D.; Zakharov, V. A.; Semikolenova, N. V.; Echevskaja, L. G.; Matsko, M. A. *Macromol. Chem. Phys.* **2008**, *209*, 2510–2515.
(38) Bryliakov, K. P.; Talsi, E. P.; Semikolenova, N. V.; Zakharov, V. A. *Organometallics* **2009**, *28*, 3225–3232.

Scheme 1. Structures of Cobalt Precatalysts Studied

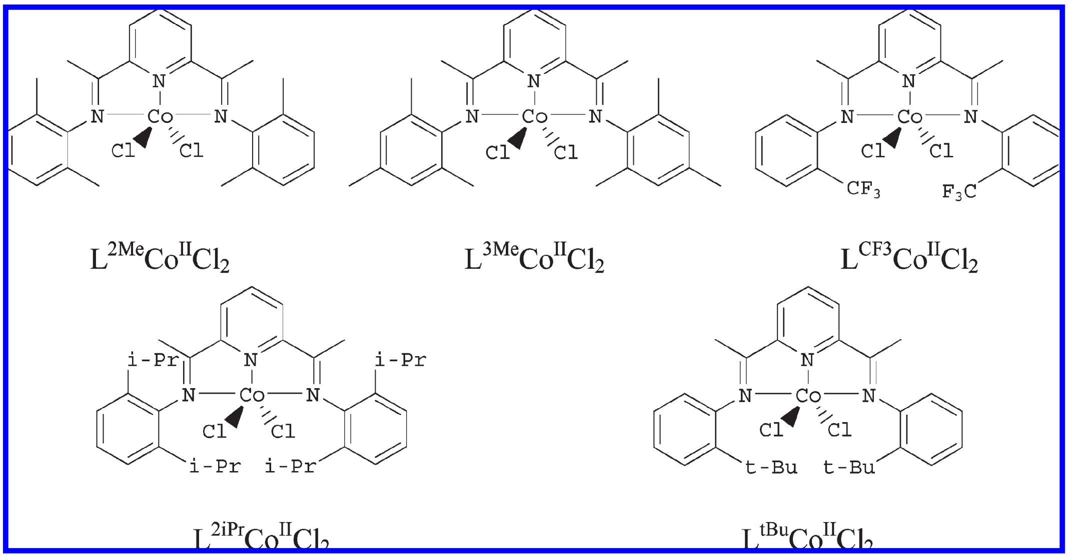

in the $LFe^{II}Cl_2$/MAO systems at [Al]/[Fe] > 500, whereas activation of $LFe^{II}Cl_2$ with $AlMe_3$ leads to neutral species of the type $L^{(\bullet-)}Fe^{(+)}(\mu\text{-}Me)_2AlMe_2$ at [Al]/[Fe] > 30, where the Fe^{II} is coordinated to the anion radical of L.[38]

As for the $LCo^{II}Cl_2$/MAO and $LCo^{II}Cl_2/AlMe_3$ analogues, the structures of the intermediates formed in these systems are more controversial. According to results of Gibson and Gal, in the $LCo^{II}Cl_2$/MAO system, initial cobalt(II) precatalyst reduction to cobalt(I) halide is followed by conversion to a cobalt(I) methyl and ultimately to a cobalt(I) cationic species. Addition of ethylene affords an ethylene adduct $[LCo^{I}(\eta\text{-}C_2H_4)]^+[\text{Me-MAO}]^-$, which is considered to be the immediate precursor to the active species.[11,21,30] In contrast, our ^1H and ^2H NMR studies of the $L^{2Me}Co^{II}Cl_2$/MAO system (Scheme 1) showed that a cobalt(II) complex with proposed structure $L^{2Me}Co^{II}Me(Cl)(MAO)$ (**1**) strongly predominates in the reaction solution at 20 °C at least several hours after mixing $L^{2Me}Co^{II}Cl_2$ and MAO.[14]

In this paper, we describe ^1H, ^2H, and ^{19}F NMR characterization of cobalt(II) and cobalt(I) species formed in the systems $LCo^{II}Cl_2$/MAO, $LCo^{II}Cl_2/AlMe_3/[CPh_3][B(C_6F_5)_4]$, and $LCo^{II}Cl_2/AlMe_3$, where L = L^{2iPr}, L^{3Me}, L^{tBu}, and L^{CF3} (Scheme 1). Correlations between the structure of the observed cobalt species and the structure of the resulting polyethylene are discussed.

Results and Discussion

Activation of $L^{2iPr}Co^{II}Cl_2$ with MAO and $AlMe_3/[CPh_3][B(C_6F_5)_4]$. The ^1H NMR spectra of the catalyst systems $L^{2iPr}Co^{II}Cl_2$/MAO ([Al]:[Co] = 100:1, [Co] = 5×10^{-3} M, toluene-d_8) and $L^{2iPr}Co^{II}Cl_2/AlMe_3/[CPh_3][B(C_6F_5)_4]$ ([Al]:[Co]:[B] = 10:1:2, [Co] = 10^{-2} M, toluene-d_8), recorded at various times after mixing the reagents at −30 to +20 °C, show that the starting cobalt complex $L^{2iPr}Co^{II}Cl_2$ quantitatively converts to cobalt(II) complexes $[L^{2iPr}Co^{II}Me(S)]^+[\text{Me-MAO}]^-$ (**2**) and $[L^{2iPr}Co^{II}Me(S)]^+[B(C_6F_5)_4]^-$ (**2′**), respectively (S = solvent or vacancy). The ^1H NMR spectra of **2** and **2′** are very similar (Figures 1a,b and Table 1). The broad peak at ca. δ 150 in the ^1H NMR spectra of **2** and **2′** belongs to a Co-CH_3 group. A similar resonance was previously observed for the related complex **1** formed in the $L^{2Me}Co^{II}Cl_2$/MAO system. Its assignment to the Co-CH_3 group was confirmed by ^2H NMR spectroscopy, using deuterated MAO.[14] As was mentioned, complex **1** was previously assigned to a neutral complex of the type $L^{2Me}Co^{II}Me(Cl)(MAO)$.[14] However, the following data provide evidence in favor of ionic structures for complexes **2**, **2′**, and **1**.

$AlMe_3/[CPh_3][B(C_6F_5)_4]$ is a well known ion pair generating reagent. The ^{19}F spectrum of **2′** is typical for an outer-sphere perfluoroaryl borate anion $[B(C_6F_5)_4]^-$ (^{19}F NMR, −20 °C: δ −134.8 ($\Delta\nu_{1/2}$ = 40 Hz), −155.0 ($\Delta\nu_{1/2}$ = 430 Hz), −165.1 ($\Delta\nu_{1/2}$ = 120 Hz)).[39,40] Hence, **2′** is the ion pair $[L^{2iPr}Co^{II}Me(S)]^+[B(C_6F_5)_4]^-$ (S = solvent or vacancy). This assumption is in agreement with recent publications of Macchioni and co-workers, demonstrating that for the post-metallocene precatalysts even with the $B(C_6F_5)_3$ activator outer-sphere ion pairs can be formed and that the vacant coordination site can be substantially unoccupied or involved in weak interaction with solvent.[41,42]

The $[B(C_6F_5)_4]^-$ counteranion of **2′** is far from the perturbing paramagnetic center, and therefore its ^{19}F chemical shifts are close to those for diamagnetic ion pairs. Apparently, the related complex **2** is the ion pair $[L^{2iPr}Co^{II}Me(S)]^+[\text{Me-MAO}]^-$. It is evident that the counteranion $[\text{Me-MAO}]^-$ is placed in the outer coordination sphere of cobalt, since in the case of the direct contact of the oligomeric molecule of $[\text{Me-MAO}]^-$ with cobalt (an inner-sphere ion pair), extremely broad ^1H resonances are expected.[43−45] The data presented show that complex **1**

---

[39] Yang, X.; Stern, C. L.; Marks, T. J. *J. Am. Chem. Soc.* **1991**, *113*, 3623.

[40] Yang, X.; Stern, C. L.; Marks, T. J. *Organometallics* **1991**, *10*, 840–842.

[41] Zuccaccia, C.; Macchioni, A.; Busico, V.; Cipullo, R.; Talarico, G.; Alfano, F.; Boone, H. W.; Frazier, K. A.; Hustad, P. D.; Stevens, J. C.; Vosejpka, P. C.; Abboud, K. A. *J. Am. Chem. Soc.* **2008**, *130*, 10354–10368.

[42] Ciancaleoni, G.; Fraldi, N.; Budzelaar, P. H. M.; Busico, V.; Macchioni,A. *Dalton Trans.* **2009**, available online.

[43] Babushkin, D. E.; Semikolenova, N. V.; Zakharov, V. A.; Talsi, E. P. *Macromol. Chem. Phys.* **2000**, *201*, 558–567.

[44] Bryliakov, K. P.; Bochmann, M.; Talsi, E. P. *Organometallics* **2004**, *23*, 149–152.

[45] Bryliakov, K. P.; Semikolenova, N. V.; Yudaev, D. V.; Zakharov, V. A.; Brintzinger, H. H.; Ystenes, M.; Rytter, E.; Talsi, E. P. *J. Organomet. Chem.* **2003**, *683*, 92–102.

previously assigned to $L^{2Me}Co^{II}Me(Cl)(MAO)$ is in reality the ion pair $[L^{2Me}Co^{II}Me(S)]^+[Me\text{-}MAO]^-$.

It is worth noting that the structure of the ion pair $[L^{2iPr}Co^{II}Me(S)]^+[Me\text{-}MAO]^-$ (**2**), formed in the $L^{2iPr}Co^{II}Cl_2$/MAO system, differs from the structure of the ion pair $[L^{2iPr}Fe^{II}(\mu\text{-}Me)_2AlMe_2]^+[Me\text{-}MAO]^-$ formed in the $L^{2iPr}Fe^{II}Cl_2$/MAO analogue.[38] In the first case, the vacant coordination site of the cobalt is unoccupied or bound by solvent (toluene), whereas in the second case this site is occupied by $AlMe_3$.

Complexes **2** and **2′** are the major cobalt species in the reaction solution even one day after mixing the reagents at 20 °C. However, prolonged storing (several days) of the samples $L^{2iPr}Co^{II}Cl_2$/MAO ([Al]:[Co] = 100:1, [Co] = 5×10^{-3} M, toluene-d_8) and $L^{2iPr}Co^{II}Cl_2/AlMe_3/[CPh_3][B(C_6F_5)_4]$ ([Al]:[Co]:[B] = 10:1:2, [Co] = 10^{-2} M, toluene-d_8) at room temperature results in the gradual decrease of the concentration of complexes **2** and **2′** and the growth of the concentration of diamagnetic cobalt(I) complexes **3** and **3′**, respectively.

^1H NMR spectra of **3** and **3′** (Figure 2, Table 1) display sharp resonances of the L^{2iPr} ligand in the range typical for diamagnetic species.

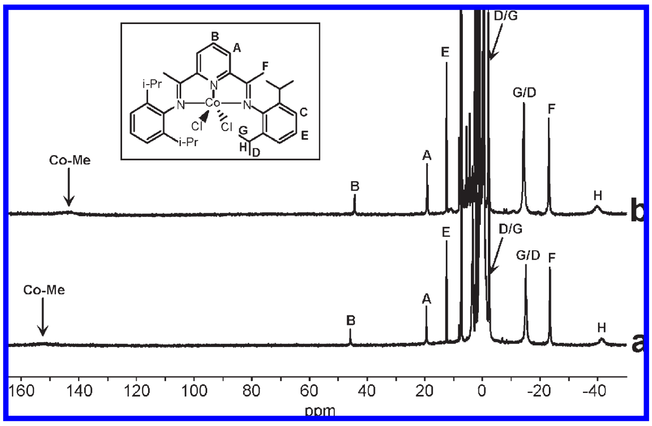

Figure 1. ^1H NMR spectra (20 °C) of the samples $L^{2iPr}Co^{II}Cl_2$/MAO ([Al]:[Co] = 100:1, [Co] = 5×10^{-3} M, toluene-d_8) (a) and $L^{2iPr}Co^{II}Cl_2/AlMe_3/[CPh_3][B(C_6F_5)_4]$ ([Al]:[Co]:[B] = 10:1:2, [Co] = 10^{-2} M, toluene-d_8) (b), recorded 16 h after mixing the reagents. The inset of the precatalyst is shown for convenience of the line assignment.

^1H NMR spectra of this type were previously reported for the ion pairs $[L^{2iPr}Co^I(\eta\text{-}C_2H_4)]^+[MeB(C_6F_5)_3]^-$ (**3_{C2H4}**) and $[L^{2iPr}Co^I(\eta\text{-}N_2)]^+[MeB(C_6F_5)_3]^-$ (**3_{N2}**) (Table 1).[21] The ^{19}F spectrum of **3′** is typical for the outer-sphere perfluoroaryl borate anion $[B(C_6F_5)_4]^-$ (^{19}F NMR, 20 °C: δ −130.2 ($\Delta\nu_{1/2}$ = 30 Hz), −161.0 ($\Delta\nu_{1/2}$ = 280 Hz), −164.1 ($\Delta\nu_{1/2}$ = 120 Hz)).[39,40] On the basis of their ^1H and ^{19}F NMR spectra, **3** and **3′** can be assigned to the ion pairs $[L^{2iPr}Co^I(S)]^+[Me\text{-}MAO]^-$ and $[L^{2iPr}Co^I(S)]^+[B(C_6F_5)_4]^-$, respectively.

The activation of $L^{2iPr}Co^{II}Cl_2$ with MAO and $AlMe_3/[CPh_3][B(C_6F_5)_4]$ at 20 °C thus results in the quantitative formation of the cobalt(II) ion pairs (**2** and **2′**), which slowly reduce to the ion pairs of cobalt(I) (**3** and **3′**) (Scheme 2).

Two weeks after the reaction onset at 20 °C, the sample $L^{2iPr}Co^{II}Cl_2$/MAO ([Al]:[Co] = 100:1, [Co] = 5×10^{-3} M, toluene-d_8) contains complexes **2** and **3** ([**2**]:[**3**] ≈ 1:1). Addition of ethylene to this sample ([Co]:[C_2H_4] = 1:25, 20 °C)

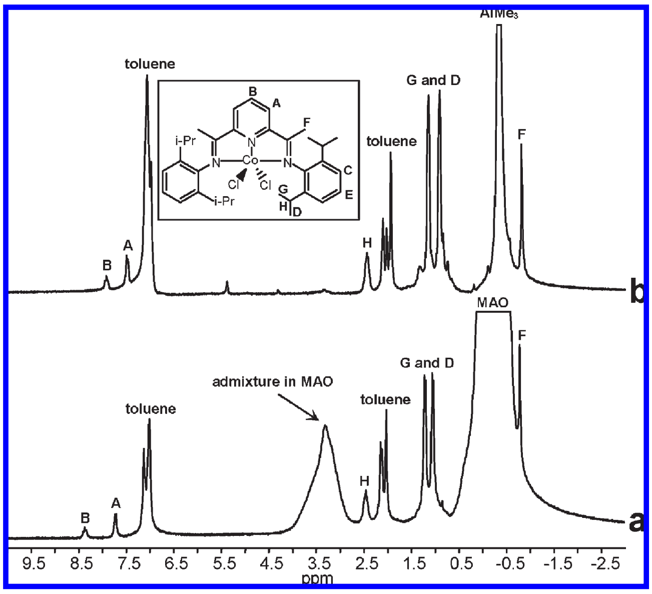

Figure 2. ^1H NMR spectra (20 °C) of the samples $L^{2iPr}Co^{II}Cl_2$/MAO ([Al]:[Co] = 100:1, [Co] = 5×10^{-3} M, toluene-d_8) 7 days after storing at room temperature (a) and $L^{2iPr}Co^{II}Cl_2/AlMe_3/[CPh_3][B(C_6F_5)_4]$ ([Al]:[Co]:[B] = 10:1:2, [Co] = 10^{-2} M, toluene-d_8) 7 days after storing at room temperature (b).

Table 1. ^1H NMR Data for the Complexes Observed upon Activation of $L^{2iPr}Co^{II}Cl_2$ with MAO, $AlMe_3/[CPh_3][B(C_6F_5)_4]$, and $AlMe_3$ (toluene-d_8, 20 °C)

		A	B	C	D	E	F	G	H		
complex		Py-*H*$_m$	Py-*H*$_p$	Ar-*H*$_m$	*Me*$_2$CH	Ar-*H*$_p$	N=C(*Me*)	*Me*$_2$CH	Me$_2$C*H*	Co-*Me*	*μ*-*Me*
$L^{2iPr}Co^{II}Cl_2$[a]		116.5	49.4	10.0	−17.8	−8.8	4.4	−19.0	−84.6		
$[L^{2iPr}Co^{II}Me(S)]^+[Me\text{-}MAO]^-$	**2**	19.4	45.9	NA	−2.4	12.4	−23.6	−15.2	−41.5	~152	
$[L^{2iPr}Co^{II}Me(S)]^+[B(C_6F_5)_4]^-$	**2′**	19.1	44.3	NA	−2.2	12.3	−23.3	−14.6	−40.0	~143	
$[L^{2iPr}Co^I(S)]^+[Me\text{-}MAO]^-$	**3**	7.71	8.35	NA	1.20	NA	−0.80	1.03	2.44		
$[L^{2iPr}Co^I(S)]^+[B(C_6F_5)_4]^-$	**3′**	7.48	7.92	NA	1.15	NA	−0.81	0.91	2.44		
$L^{2iPr}Co^I(\mu\text{-}Me)(\mu\text{-}Cl)AlMe_2$[b]	**4a**	NA	8.1	NA	NA	NA	−0.07	0.8	3.1		−1.6
$L^{2iPr}Co^I(\mu\text{-}Me)_2AlMe_2$[b]	**4b**	7.5	9.7	NA	1.1	NA	N/O	0.6	3.1		−2.8
$[L^{2iPr}Co^I(\eta\text{-}C_2H_4)]^+[AlMe_3Cl]^-$[b]	**5**	NA	8.1	NA	1.1	NA	0.6	0.8	3.1		
$[L^{2iPr}Co^I(\eta\text{-}N_2)]^+[MeB(C_6F_5)_3]^-$[c]	**3_{N2}**	6.69	7.55	6.87	1.05	7.00	1.11	0.98	2.85		N/O
$[L^{2iPr}Co^I(\eta\text{-}C_2H_4)]^+[MeB(C_6F_5)_3]^-$[c]	**3_{C2H4}**	~7.0	8.00	6.77	1.09	~7.0	0.75	0.76	3.02		N/O
$L^{2iPr}Co^IMe$[c]		7.86	10.19	7.37	1.19	7.49	−1.14	0.62	3.13	N/O	
$L^{2iPr}Co^ICl$[c]		6.91	9.54	7.27	1.18	7.41	0.05	1.06	3.33		

[a] Solution in CH_2Cl_2. [b] Spectra recorded at −10 °C, only broad singlets in the each case. [c] The data are from ref 21. N/O, not observed. NA, not reliably assigned.

leads to ethylene polymerization, monitored by the decrease of the ethylene peak at δ 5.2. In addition, the resonances of **2** disappear and only **3** is observed in the sample containing ethylene. Hence, ethylene induces the rapid reduction of **2** into **3**. Thus, in agreement with the previous assumption,[11,21] the cobalt(I) species seems to be the active polymerizing species in the catalyst systems $LCo^{II}Cl_2/MAO$. However, the quantitative conversion of cobalt(II) to cobalt(I) occurs only in the presence of monomer.

Activation of $L^{2iPr}Co^{II}Cl_2$ with $AlMe_3$. In contrast to the $L^{2iPr}Co^{II}Cl_2/MAO$ and $L^{2iPr}Co^{II}Cl_2/AlMe_3/[CPh_3][B(C_6F_5)_4]$ systems, where cobalt(II) species predominate in the reaction solution at least several hours after the reaction onset, the activation of $L^{2iPr}Co^{II}Cl_2$ with $AlMe_3$ ([Al]:[Co] = 4:1, [Co] = 10^{-2} M, toluene-d_8) leads to a very rapid and quantitative reduction of the starting complex $L^{2iPr}Co^{II}Cl_2$ to two types of diamagnetic complexes of cobalt(I), denoted as **4a** and **4b** (Figure 3a, Table 1). On the basis of the previous studies of Gibson and Gal,[11,21] one can expect that complexes $L^{2iPr}Co^{I}Me$ and/or $L^{2iPr}Co^{I}Cl$ are formed in the $L^{2iPr}Co^{II}Cl_2/AlMe_3$ system. However, the ^1H NNR spectra of **4a** and **4b** differ from those of $L^{2iPr}Co^{I}Me$ and $L^{2iPr}Co^{I}Cl$ (Table 1). We have proposed that **4a** and **4b** are adducts of the type $L^{2iPr}Co^{I}(\mu\text{-}Me)(\mu\text{-}Cl)AlMe_2$ (**4a**) and $L^{2iPr}Co^{I}(\mu\text{-}Me)_2AlMe_2$ (**4b**). In agreement with this prediction, only **4b** was observed in the sample $L^{2iPr}CoCl_2/AlMe_3$ with a [Al]:[Co] ratio of 50.

The ^1H NMR spectrum of Figure 3a displays two low-field resonances at δ −1.6 and −2.8. The sample containing only **4b** exhibits only the one signal at δ −2.8. The latter signal can be attributed to the μ-Me group of **4b**, and the signal at δ −1.6 to a μ-Me group of **4a**. To support this assignment, the ^2H NMR spectrum of the system $L^{2iPr}Co^{II}Cl_2/Al(CD_3)_3$ ([Al]:[Co] = 6:1, [Co] = 2×10^{-2} M, toluene) was recorded. This spectrum exhibits resonances at δ −1.7 and −3.0, identical within accuracy of our measurements to those observed in the ^1H NMR spectrum. Thus, **4a** and **4b** are neutral cobalt(I) species of the type $L^{2iPr}Co^{I}(\mu\text{-}Me)(\mu\text{-}Cl)AlMe_2$ and $L^{2iPr}Co^{I}(\mu\text{-}Me)_2AlMe_2$ (Scheme 2).

Complexes **4a** and **4b** are unstable and rapidly (within several minutes) decay at 20 °C via transfer of the L^{2iPr} ligand to aluminum to afford the paramagnetic complex $[L^{2iPr(\bullet-)}Al^{(+)}Me_2]$, exhibiting an EPR signal at g = 2.003 (Figure 4). This complex was first discovered by Gambarotta and co-workers.[24] It is formulated as a complex of Al^{III} with the anion radical of $L^{2iPr(\bullet-)}$ and two Me anions. The EPR spectrum of Figure 4 displays partially resolved multiline hyperfine splitting (hfs) from Al, N, and H nuclei (inset). This

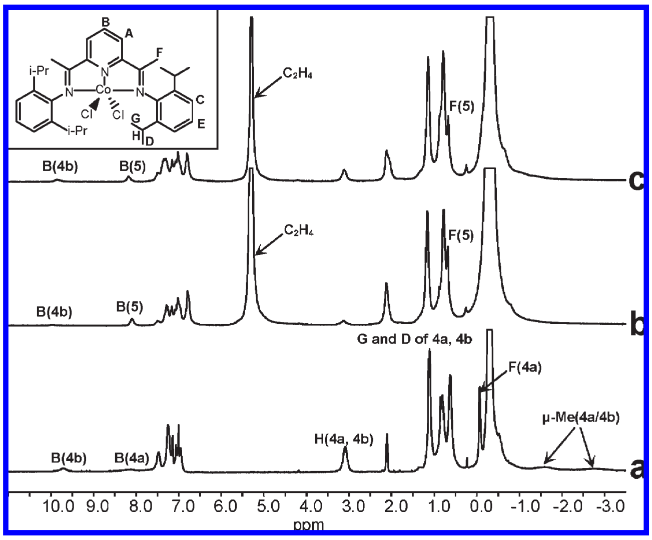

Figure 3. ^1H NMR spectra of the samples $L^{2iPr}Co^{II}Cl_2/AlMe_3$ ([Al]:[Co] = 4:1) (a) and $L^{2iPr}Co^{II}Cl_2/AlMe_3/C_2H_4$ ([Al]:[Co]:[C_2H_4] = 10:1:50) (b) recorded 10 min after mixing the reagents ([Co] = 10^{-2} M, toluene-d_8, −20 °C). Sample in "b" 10 min after additional storing at −10 °C (c).

Scheme 2. Interaction of $L^{2iPr}Co^{II}Cl_2$ with MAO, $AlMe_3/[CPh_3][B(C_6F_5)_4]$, and $AlMe_3$

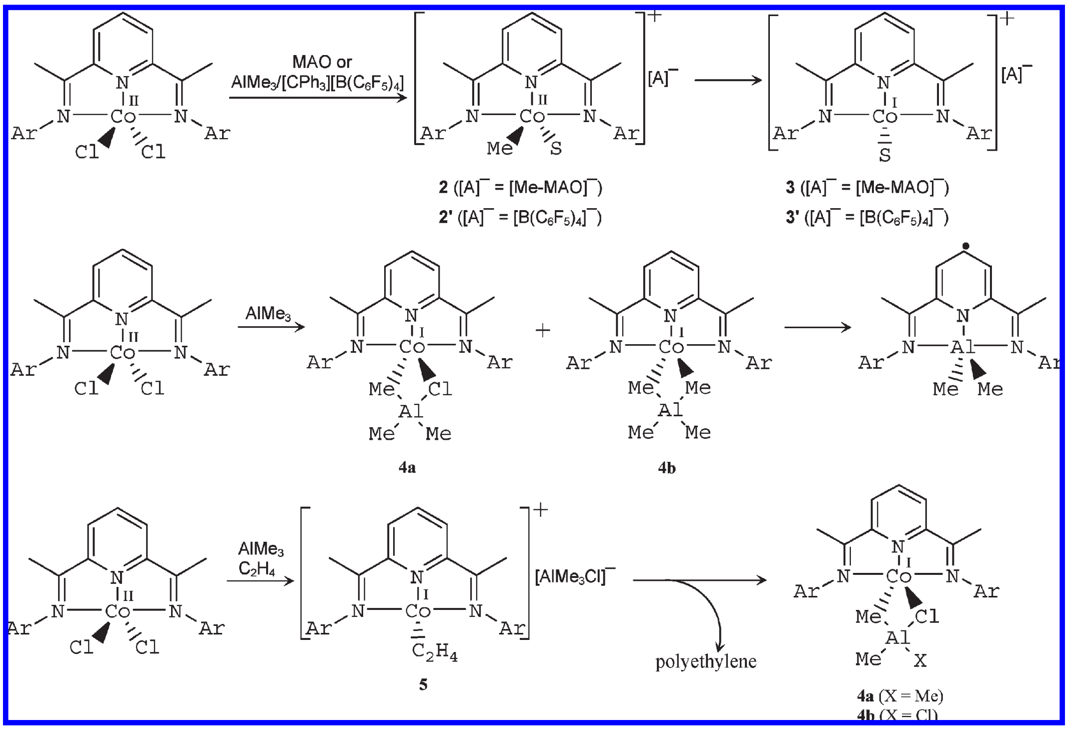

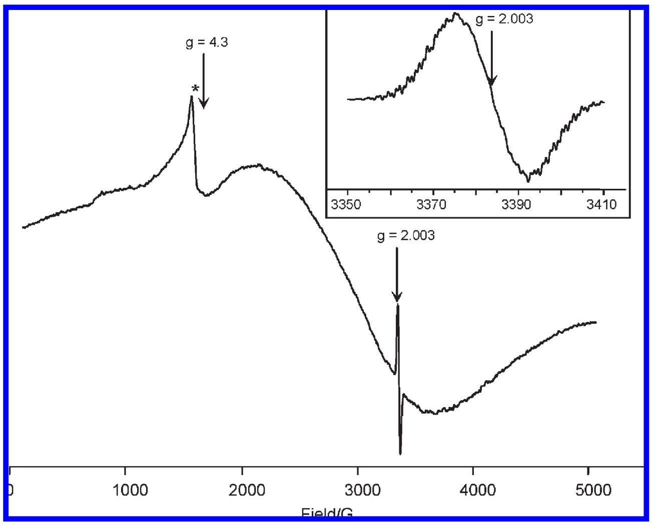

Figure 4. EPR spectrum (−196 °C) of the sample $L^{2iPr}Co^{II}Cl_2$/$AlMe_3$ ([Al]:[Co] = 4:1, toluene-d_8, [Co] = 5×10^{-3} M) after 1 day storage at room temperature (asterisk marks signal of an impurity in the sample tube).

splitting has been previously well resolved and interpreted for the same aluminum complex formed upon reacting the ligand, L^{2iPr}, with $AlMe_3$.[24]

The EPR spectrum of Figure 4 also displays a very broad and intense resonance ($\Delta H_{1/2}$ = 1700 G) from the ferromagnetic cobalt(0) species. Apparently, cobalt(I) compounds reduce at 20 °C to metallic cobalt. The black cobalt(0) residue was observed in the NMR tube upon storing the $L^{2iPr}Co^{II}Cl_2$/$AlMe_3$ sample during 1 h at 20 °C.

Interestingly, complexes **4a** and **4b** predominate in the sample $L^{2iPr}Co^{II}Cl_2$/$AlMe_3$ only in the absence of monomer. The ^{1}H NMR spectrum of the sample $L^{2iPr}Co^{II}Cl_2$/$AlMe_3$/C_2H_4 ([Al]:[Co]:[C_2H_4] = 10:1:50) recorded just after mixing the reagents at −20 °C displays resonances of the new complex **5** with chemical shifts close to those for the ion pair $[L^{2iPr}Co^{I}(\eta\text{-}C_2H_4)]^+[MeB(C_6F_5)_3]^-$ ($\mathbf{3_{C2H4}}$). The resonances of **4a** (**4b**) were also observed (Figure 3b, Table 1). On the basis of the similarity of the ^{1}H NMR spectra of **5** and $\mathbf{3_{C2H4}}$, complex **5** can be assigned to the ion pair $[L^{2iPr}Co^{I}(\eta\text{-}C_2H_4)]^+[AlMe_3Cl]^-$ (Scheme 2). According to EPR spin-trap studies, the Lewis acidity of $AlEt_2Cl$ is higher than that of MAO.[46] Therefore, the abstraction of methide anion by in situ formed $AlMe_2Cl$ and formation of the ion pair **5** seem to be plausible. The decrease of ethylene concentration in the course of polymerization leads to the decrease in concentration of **5** and the growth in concentration of **4a** (**4b**) (Figure 3c).

Activation of $L^{3Me}Co^{II}Cl_2$ with MAO, $AlMe_3$/$[CPh_3][B(C_6F_5)_4]$, and $AlMe_3$. The ^{1}H NMR spectrum of the catalyst system $L^{3Me}Co^{II}Cl_2$/MAO ([Al]:[Co] = 100:1, [Co] = 6×10^{-3} M, toluene-d_8) recorded 5 min after mixing the reagents at −20 °C displays resonances of two types of cobalt(II) complexes (complexes **6** and **7**, Figure 5a and Table 2).

Warming the sample to 20 °C leads to the disappearance of complex **6**, and only complex **7** is observed (Figure 5b). The ^{1}H NMR spectrum of **7** resembles that of **2** (Tables 1 and 2).

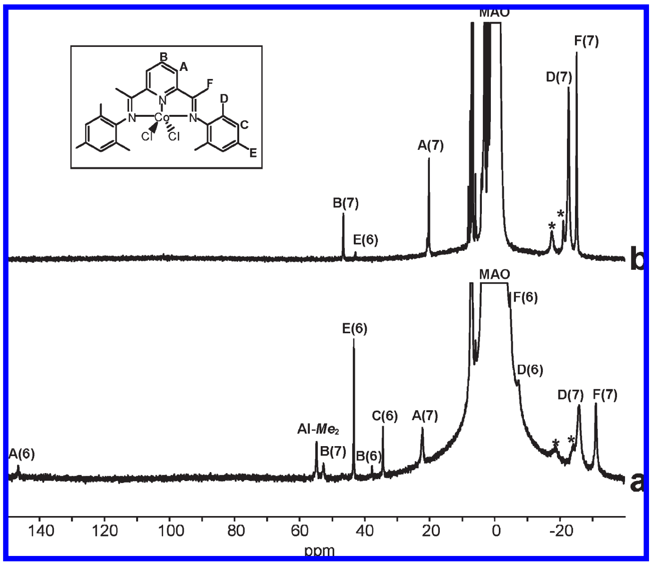

Figure 5. ^{1}H NMR spectra of the $L^{3Me}LCo^{II}Cl_2$/MAO ([Al]:[Co] = 100:1, [Co] = 6×10^{-3} M, toluene-d_8) at −20 °C (a) and at 20 °C (b). Asterisks mark still unidentified species, probably outer-sphere ion pairs, containing a Co-Cl instead of a Co-Me moiety.

Therefore, **7** is the outer-sphere ion pair $[L^{3Me}Co^{II}(Me)(S)]^+$-$[Me\text{-}MAO]^-$. Complex **6** displays a resonance at δ = 52.5 (6H), characteristic of the $AlMe_2$ moiety in the heterobinuclear ion pairs $[LFe^{II}(\mu\text{-}Me)_2AlMe_2]^+[Me\text{-}MAO]^-$[10] (Figure 5a and Table 2). Hence, **6** is the heterobinuclear ion pair $[L^{3Me}Co^{II}(\mu\text{-}Me)_2AlMe_2]^+[Me\text{-}MAO]^-$ (Scheme 3).

Thus, the nature of the substituents in the aryl rings of the bis(imino)pyridine ligand can affect the tendency of the $[LCo^{II}Me]^+$ cation to bind the particular donor atom. For the $L^{2iPr}Co^{II}Cl_2$/MAO system, the structure $[L^{2iPr}Co^{II}Me\text{-}(S)]^+[Me\text{-}MAO]^-$ (S = solvent or vacancy) is preferable at both low and high temperatures, whereas for the L^{3Me}-$Co^{II}Cl_2$/MAO analogue, the structure $[L^{3Me}Co^{II}Me(S)]^+$-$[Me\text{-}MAO]^-$ is preferable at high temperatures, and the structure $[L^{3Me}Co^{II}(\mu\text{-}Me)_2AlMe_2]^+[Me\text{-}MAO]^-$ at low temperatures.

In the system $L^{3Me}Co^{II}Cl_2$/$AlMe_3$/$[CPh_3][B(C_6F_5)_4]$ ([Al]:[Co]:[B] = 10:1:1, [Co] = 10^{-2} M, toluene-d_8), the heterobinuclear ion pair $[L^{3Me}Co^{II}(\mu\text{-}Me)_2AlMe_2]^+[B(C_6F_5)_4]^-$ (**6′**) is the major species in the reaction solution at both relatively low (−20 °C) and high (20 °C) temperatures (Figure 6, Table 2). Probably $[B(C_6F_5)_4]^-$ is a less bulky counterion than $[Me\text{-}MAO]^-$ and favors coordination of $AlMe_3$ to the $[L^{3Me}Co^{II}Me]^+$ cation. The minor signals in Figures 6(a, b) belong to the ion pair $[L^{3Me}Co^{II}Me(S)]^+$-$[B(C_6F_5)_4]^-$ (**7′**).

The ion pairs **6** (**6′**) and **7** (**7′**), similar to the ion pairs **2** and **2′**, reduce at 20 °C to the ion pairs of cobalt(I) (**8** and **8′**, Table 2). The following structures for these ion pairs can be suggested: $[L^{3Me}Co^{I}(S)]^+[Me\text{-}MAO]^-$ (**8**) and $[L^{3Me}Co^{I}\text{-}(S)]^+[B(C_6F_5)_4]^-$ (**8′**). Ion pairs **8** and **8′** are stable at room temperature.

The interaction of $L^{3Me}Co^{II}Cl_2$ with $AlMe_3$ at −10 °C leads to reduction of the cobalt(II) and the formation of two complexes of cobalt(I). On the basis of their ^{1}H NMR spectra, they can be assigned to the neutral complexes $L^{3Me}Co^{I}(\mu\text{-}Me)(\mu\text{-}Cl)AlMe_2$ (**9a**) and $L^{3Me}Co^{I}(\mu\text{-}Me)_2Al\text{-}Me_2$ (**9b**). As in the case of the $L^{2iPr}Co^{II}Cl_2$/$AlMe_3$ system,

---

(46) Talsi, E. P.; Semikolenova, N. V.; Panchenko, V. N.; Sobolev, A. P.; Babushkin, D. E.; Shubin, A. A.; Zakharov, V. A. *J. Mol. Catal. A* **1999**, *139*, 131–137.

Table 2. ^{1}H NMR Data for the Complexes Observed upon Activation of $L^{3Me}Co^{II}Cl_2$ with MAO, $AlMe_3/[CPh_3][B(C_6F_5)_4]$, and $AlMe_3$ (toluene-d_8)

			A	B	C	D	E	F		
complex		T, °C	Py-H_m	Py-H_p	Ar-H_m	Ar-Me_o	Ar-Me_p	N=C(Me)	Co-Me	AlMe_2
$L^{3Me}Co^{II}Cl_2$[a]		+20	110.7	36.3	6.5	−26.5	17.0	−0.5		
$L^{3Me}Co^{II}Cl_2$[a]		−20	141.5	49.3	6.5	−38.1	21.5	−0.5		
$[L^{3Me}Co^{II}(\mu\text{-Me})_2AlMe_2]^+[Me\text{-}MAO]^-$	**6**	−20	147.6	37.5	34.4	−7.9	43.4	−5.6	N/O	55.2
$[L^{3Me}Co^{II}(\mu\text{-Me})_2AlMe_2]^+[B(C_6F_5)_4]^-$	**6′**	−20	147.8	36.3	35.3	−8.1	43.4	−3.9	N/O	57.2
$[L^{3Me}Co^{II}Me(S)]^+[Me\text{-}MAO]^-$	**7**	−20	21.7	52.0	NA	−26.3	NA	−31.7	N/O[b]	
		+20	20.2	46.4	NA	−22.5	NA	−24.9	N/O[b]	
$[L^{3Me}Co^{II}Me(S)]^+[B(C_6F_5)_4]^-$	**7′**	−20	21.6	50.4	NA	−25.5	NA	−30.6	N/O	
$[L^{3Me}Co^{I}(S)]^+[Me\text{-}MAO]^-$	**8**	+20	7.61	8.19	6.71	1.88	1.86	−0.71		
$[L^{3Me}Co^{I}(S)]^+[B(C_6F_5)_4]^-$	**8′**	+20	7.42	7.89	6.66	1.80	1.76	−0.72		
$L^{3Me}Co^{I}(\mu\text{-Me})(\mu\text{-Cl})AlMe_2$	**9a**	+10	7.5	12.2	6.78	1.52	2.43	−1.64	N/O	N/O
$L^{3Me}Co^{I}(\mu\text{-Me})_2AlMe_2$	**9b**	+10	7.6	12.6	6.82	1.41	2.43	−1.85	N/O	N/O
$[L^{3Me}Co^{I}(\eta\text{-}C_2H_4)]^+[AlMe_3Cl]^-$	**10**	+10	7.2	8.35	6.54	1.57	2.03	0.36		
$L^{3Me}Co^{I}Me$[c]		+20	7.88	10.08	6.99	1.93	2.28	−1.21	0.46	
$L^{3Me}Co^{I}Cl$[c]		+20	6.90	9.49	6.93	2.19	2.18	−0.06		

[a] Solution in CH_2Cl_2. [b] A broad singlet ($\delta \approx 171$, $\Delta\nu_{1/2} \approx 600$ Hz) was observed at 0 °C after prolonged ^{1}H NMR spectrum accumulation. [c] The data are from ref 21. N/O, not observed. NA, not reliably assigned.

Scheme 3. Interaction of $L^{3Me}Co^{II}Cl_2$ with MAO, $AlMe_3/[CPh_3][B(C_6F_5)_4]$, and $AlMe_3$

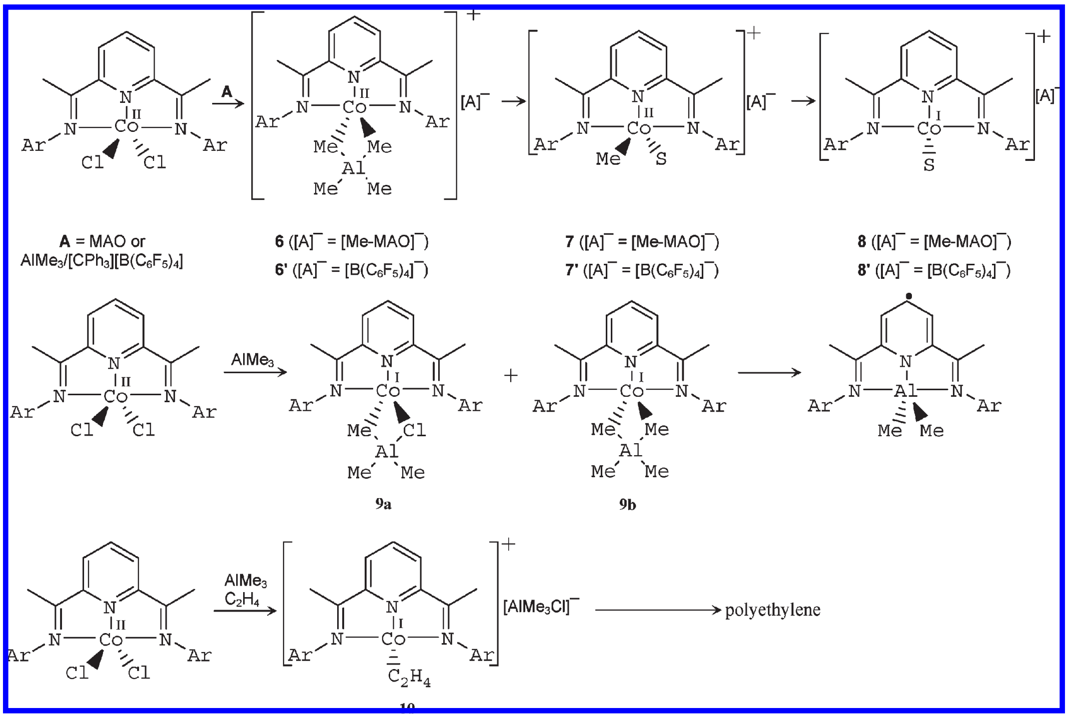

in the presence of ethylene, the formation of the new complex **10**, with proposed structure $[L^{3Me}Co^{I}(\eta\text{-}C_2H_4)]^+[AlMe_3Cl]^-$, is observed (Table 2, Scheme 3).

Activation of $L^{tBu}Co^{II}Cl_2$ with MAO, $AlMe_3/[CPh_3][B(C_6F_5)_4]$, and $AlMe_3$. Complexes observed in the systems $L^{tBu}Co^{II}Cl_2$/MAO and $L^{tBu}Co^{II}Cl_2/AlMe_3/[CPh_3][B(C_6F_5)_4]$ are similar to those observed in the systems $L^{3Me}Co^{II}Cl_2$/MAO and $L^{3Me}Co^{II}Cl_2/AlMe_3/[CPh_3][B(C_6F_5)_4]$. Their structures are presented in Scheme 4, and the parameters of their ^{1}H NMR spectra are collected in Table 3.

Activation of $L^{tBu}Co^{II}Cl_2$ with $AlMe_3$ affords diamagnetic complexes of cobalt(I), the ^{1}H NMR resonances of which are broadened and less well resolved than in the case of $L^{2iPr}Co^{II}Cl_2$ and $L^{3Me}Co^{II}Cl_2$ precatalysts. This precludes their assignment; however, addition of ethylene to the sample $L^{tBu}Co^{II}Cl_2/AlMe_3$ results in the formation of complex **14** with well-resolved signals, which can be attributed to the ion pair $[L^{tBu}Co^{I}(\eta\text{-}C_2H_4)]^+[AlMe_3Cl]^-$ (Table 3).

Activation of $L^{CF3}CoCl_2$ with MAO, $AlMe_3/[CPh_3][B(C_6F_5)_4]$, and $AlMe_3$. The ^{1}H NMR spectra of the system $L^{CF3}Co^{II}Cl_2$/MAO show that the ion pair $[L^{CF3}Co^{II}(\mu\text{-Me})_2AlMe_2]^+[Me\text{-}MAO]^-$ (**15**) is formed at the initial stage of activation at low temperatures (Figure 7a, Table 4). In contrast to the MAO-based systems considered above, the heterobinuclear ion pair **15** does not convert to an ion pair of the type $[LCo^{II}Me(S)]^+[Me\text{-}MAO]^-$ at room temperature. The half-life of **15** amounts to 1 h at 20 °C. Thus, in the case of $L = L^{CF3}$, coordination of $AlMe_3$ to the cation $[LCo^{II}Me]^+$ is more favorable than in the case of $L = L^{2iPr}$, L^{3Me}, and L^{tBu}. Such precatalysts activated with MAO display only the resonances of the ion pairs $[LCo^{II}Me(S)]^+[Me\text{-}MAO]^-$ at 20 °C.

Cobalt(II) species formed in the $L^{CF3}Co^{II}Cl_2$/MAO system reduce with time into their cobalt(I) counterparts.

However, the assignment of their ^{1}H NMR resonances is complicated by line broadening caused by rapid reduction of the monovalent cobalt to ferromagnetic cobalt(0). Thus, cobalt(I) species formed in the $L^{CF3}Co^{II}Cl_2$/MAO system are less stable to degradation than those formed in the case of the L = L^{2iPr}, L^{3Me}, and L^{tBu} analogues.

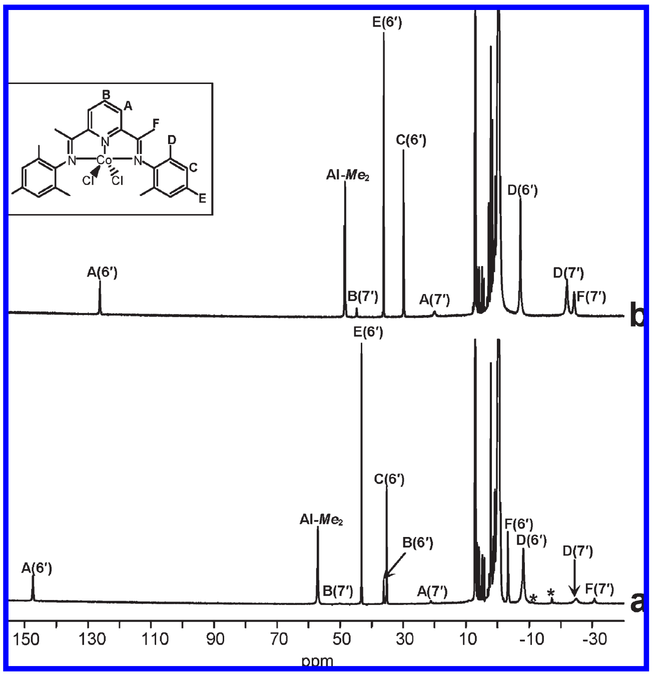

Figure 6. ^{1}H NMR spectra of the $L^{3Me}Co^{II}Cl_2/AlMe_3/[CPh_3][B(C_6F_5)_4]$ system ([Al]:[Co]:[B] = 10:1:1, [Co] = 10^{-2} M, toluene-d_8) at −20 °C (a) and at 20 °C (b). Asterisks mark still unidentified signals.

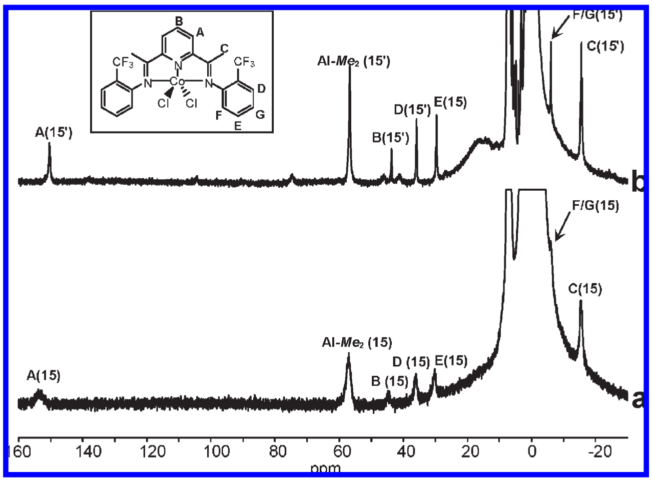

Figure 7. ^{1}H NMR spectra (−40 °C) of the samples $L^{CF3}Co^{II}Cl_2$/MAO ([Al]:[Co] = 100:1, [Co] = 5×10^{-3} M, toluene-d_8) (a) and $L^{CF3}Co^{II}Cl_2/AlMe_3/[CPh_3][B(C_6F_5)_4]$ ([Al]:[Co]:[B] = 10:1:2, [Co] = 10^{-2} M, toluene-d_8) (b) 30 min after storing at −40 °C.

Scheme 4. Structures of the Cobalt Species Formed upon Activation of $L^{tBu}Co^{II}Cl_2$ with MAO, $AlMe_3/[CPh_3][B(C_6F_5)_4]$, and $AlMe_3/C_2H_4$

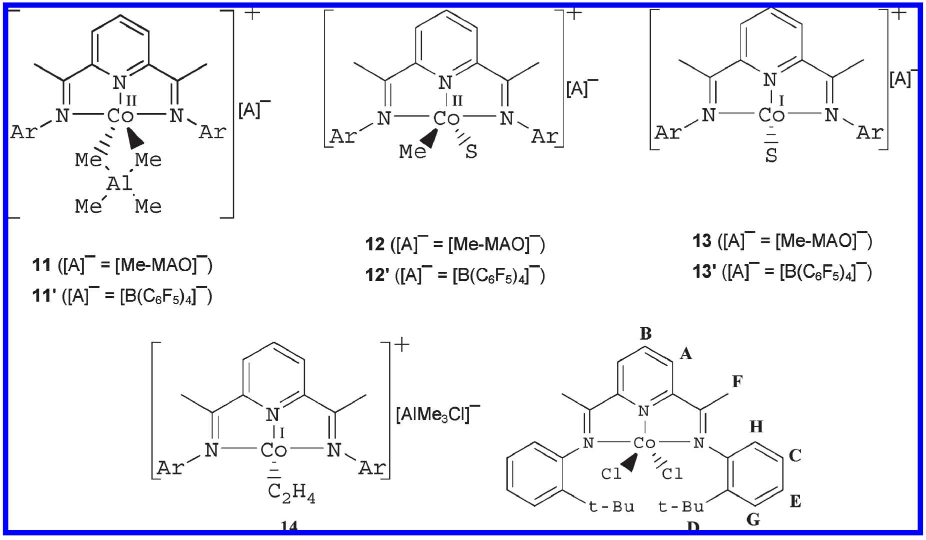

Table 3. ^{1}H NMR Data for the Complexes Observed upon $L^{tBu}Co^{II}Cl_2$ Activation with MAO, $AlMe_3$, and $AlMe_3/[CPh_3][B(C_6F_5)_4]$ (toluene-d_8)

			A	B	C	D	E	F	G	H		
complex		*T*, °C	Py-*H*$_m$	Py-*H*$_p$	Ar-*H*	C(*CH*$_3$)$_3$	Ar-*H*	N=C(*Me*)	Ar-*H*	Ar-*H*	Co-*Me*	Al*Me*$_2$
$[L^{tBu}Co^{II}(\mu\text{-}Me)_2AlMe_2]^+[Me\text{-}MAO]^-$	**11**	−20	138.6	44.1	30.7	−35.8	−6.0	−10.1	29.8	NA	N/O	48.3
$[L^{tBu}Co^{II}Me(S)]^+[Me\text{-}MAO]^-$	**12**	−20	~17.6	~51.4	NA	−14.7	NA	−32.8	NA	NA	N/O	
		+20	16.5	44.6	NA	−12.7	NA	−26.5	NA	NA	~139	
$[L^{tBu}Co^{II}(\mu\text{-}Me)_2AlMe_2]^+[B(C_6F_5)_4]^-$	**11′**	−20	140.2	44.6	31.0	−36.4	−6.3	−10.6	29.7	NA	N/O	48.9
		+20	118.3	37.7	26.9	−28.7	−4.8	−8.2	25.6	NA	N/O	40.9
$[L^{tBu}Co^{II}Me(S)]^+[B(C_6F_5)_4]^-$	**12′**	+20	16.5	44.3	NA	−13.2	NA	−26.2	NA	NA	N/O	
$[L^{tBu}Co^{I}(S)]^+[Me\text{-}MAO]^-$	**13**	+20	7.64	8.27	NA	1.17/1.14	NA	−0.70	7.23	6.63		
$[L^{tBu}Co^{I}(\eta\text{-}C_2H_4)]^+[AlMe_3Cl]^{-a}$	**14**	−30	7.21	8.03	NA	0.79	NA	0.85	NA	NA		

[a] The signal of η-C_2H_4 at δ 4.82 was observed. N/O, not observed. NA, not reliably assigned.

Table 4. ^{1}H NMR Data for the Complexes Observed upon Activation of $L^{CF3}Co^{II}Cl_2$ with MAO and $AlMe_3/[CPh_3][B(C_6F_5)_4]$ (toluene-d_8)

			A	B	C	D	E	F	G	
complex		T, °C	Py-H_m	Py-H_p	N=C(Me)	Ar-H_m	Ar-H_m	Ar-H	Ar-H	AlMe_2
$L^{CF3}Co^{II}Cl_2$[a]		−40	158.3	67.9	13.6	17.8	−4.5;	−16.4;	NA	
		+20	113.8	47.1	9.3	14.4	−4.0	−10.3	NA	
$[L^{CF3}Co^{II}(\mu\text{-}Me)_2AlMe_2]^+[Me\text{-}MAO]^-$	**15**	−40	156.7	45.8	−16.1	37.0	31.0	−6.3	NA	58.5
		+20	114.9	37.4	−8.4	24.7	23.8	−5.9	10.3	38.8
$[L^{CF3}Co^{II}(\mu\text{-}Me)_2AlMe_2]^+[B(C_6F_5)_4]^-$	**15′**	−40	150.3	43.6	−15.6	35.8	29.5	−6.2	NA	56.7

[a] Solution in $CDCl_3$. N/O, not observed. NA, not reliably assigned.

Table 5. Ethylene Polymerization Data for $LCo^{II}Cl_2$ Complexes with Different Activators[a]

							content per PE molecule [d]	
run	complex	activator	yield [b]	initial activity [c]	$M_w \times 10^{-3}$	M_w/M_n	$-CH_3$	$-CH{=}CH_2$
1	$L^{2iPr}CoCl_2$	MAO	1250	170	18	2.0	0.8	1.0
2		$AlMe_3$	750	140	18	2.0	0.8	1.0
3		$AlMe_3$/"B" [e]	980	110	18	2.0	0.9	1.0
4	$L^{3Me}CoCl_2$	MAO	5880	550	1.7	1.8	1.0	1.0
5		MAO (20)	2400	300	1.7	1.9	1.0	1.0
6		$AlMe_3$	1920	235	1.4	2.6	1.0	1.0
7		$AlMe_3$/"B"	1210	175	1.2	1.7	1.0	1.0
8	$L^{tBu}CoCl_2$	MAO	4500	480	330	2.5	1.0	1.0
9		$AlMe_3$	2100	370	420	3.9	1.0	1.0
10	$L^{CF3}CoCl_2$	MAO	2700[f]	620				
11		$AlMe_3$	1600[f]	430				
12 [g]	$L^{2Me}CoCl_2$	MAO	3100	80	1.5	1.8	1.0	1.0
13 [g]		$AlMe_3$	3600	60	1.6	1.8	1.0	1.0

[a] Polymerization in toluene at 40 °C, ethylene pressure 5 bar (runs 4 and 8, 2 bar), for 30 min, [Co] = 1.4×10^{-5} M, [Al]:[Co] = 500:1. [b] kg PE·mol(Co)$^{-1}$·bar^{-1}. [c] Initial activity, calculated from the PE yield for 2 min of polymerization, in kg PE·mol(Co)$^{-1}$·bar^{-1}·min^{-1}. [d] IR spectroscopy data (for runs 4−7 ^{13}C NMR data). [e] "B" = $[CPh_3][B(C_6F_5)_4]$ (molar ratio [Co]:[Al]:[B] = 1:100:1). [f] Liquid oligomers were obtained. [g] Data of ref 47.

The ^{1}H NMR spectrum of the catalyst system $L^{CF3}Co^{II}Cl_2/AlMe_3/[CPh_3][B(C_6F_5)_4]$ recorded 30 min after reaction onset at −40 °C is similar to that observed for the system $L^{CF3}Co^{II}Cl_2$/MAO at this temperature and belongs to the ion pair $[L^{CF3}Co^{II}(\mu\text{-}Me)_2AlMe_2]^+[B(C_6F_5)_4]^-$ (**15′**) (Figure 7b, Table 4). This ion pair decays with the half-life of 40 min at 0 °C. The decay is accompanied by the broadening of NMR peaks due to the appearance of cobalt(0) species. Hence, the cobalt species formed in the system $L^{CF3}Co^{II}Cl_2/AlMe_3/[CPh_3][B(C_6F_5)_4]$ are more prone to reduction than their analogues formed in other $LCo^{II}Cl_2/AlMe_3/[CPh_3][B(C_6F_5)_4]$ systems studied. The attempts to identify cobalt(I) species formed in the systems based on L = L^{CF3} were unsuccessful due to the line broadening. Any attempts to study these systems by ^{19}F NMR were unsuccessful.

Correlation of Polymerization and NMR Spectroscopic Data. Data on the catalyst activity for ethylene polymerization by $LCo^{II}Cl_2$ (L = L^{2iPr}, L^{tBu}, L^{3Me}) complexes with different activators and the characteristics of the obtained PE samples are collected in Table 5 and Figures 8−11. Like most homogeneous catalysts, the studied systems demonstrate high initial activity that decreases with the increase in polymerization time (Figures 8 and 9). It is possible to distinguish two sections on the kinetic curves: a very sharp drop of the polymerization rate in the first minute of polymerization time and a much more gradual decrease with further duration of the reaction that leads to high yield of the PE in prolonged (30 min) polymerization runs. The value of the initial activity (Table 5) and the deactivation rate depend on the cobalt complex composition (Figure 8). The activator nature weakly affects the shape of the kinetic curve for polymerization over the studied catalysts (Figure 9).

The catalyst systems based on $LCo^{II}Cl_2$ (L = L^{2iPr}, L^{tBu}, L^{3Me}) produce highly linear PE containing about one $-CH_3$ and one $-CH{=}CH_2$ group per one PE molecule. The molecular mass of the PE samples obtained with $LCo^{II}Cl_2$ depends on the composition of bis(imino)pyridine ligand: with the increase of the steric bulk of a substituent at the *ortho*-aryl position the MM of the produced PE also increases (Table 5).

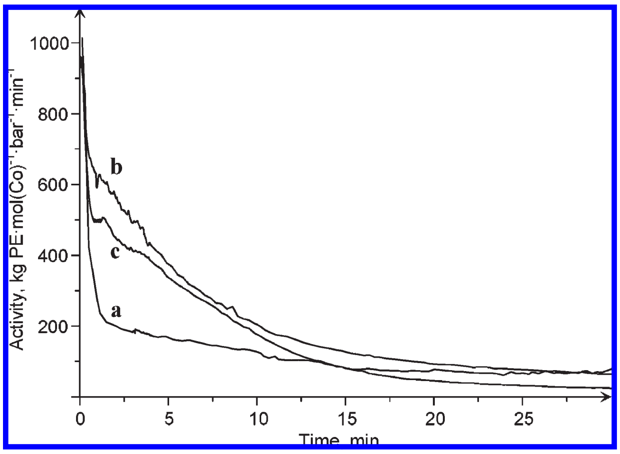

Figure 8. Rate of the ethylene polymerization vs time for $L^{2iPr}Co^{II}Cl_2$ (a), $L^{3Me}Co^{II}Cl_2$ (b), and $L^{tBu}Co^{II}Cl_2$ (c), activated with MAO (runs 1, 4, and 8 in Table 5).

The obtained PE samples are characterized with rather narrow molecular mass distribution (M_w/M_n was close to 2), depending on the composition of the cobalt complex, the activator nature, and the polymerization conditions.

Similar results were obtained for earlier[14,47] studied catalyst systems, based on $LCo^{II}Cl_2$ (L = L^{2Me}). The molecular structure of the isolated polymers (Table 5, runs 12 and 13) was close to those obtained with the catalysts based on the $L^{3Me}Co^{II}Cl_2$ complex (Table 5, runs 4 and 6).

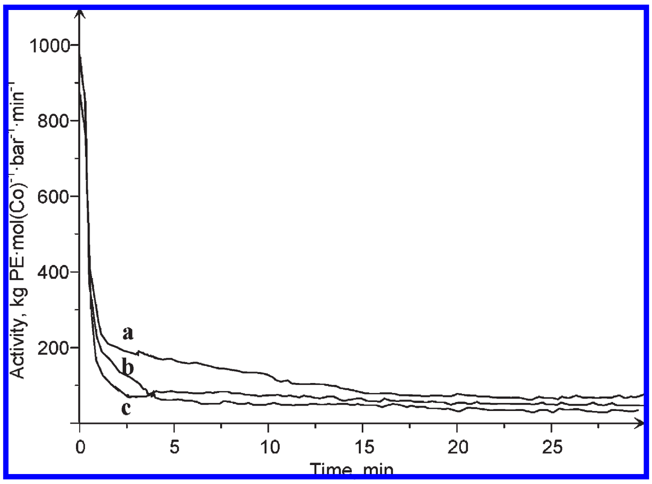

Figure 9. Rate of the ethylene polymerization vs time for $L^{2iPr}Co^{II}Cl_2$, activated with MAO (a), $AlMe_3$ (b), and $AlMe_3$/"B" (c) (runs 1, 2, and 3 in Table 5).

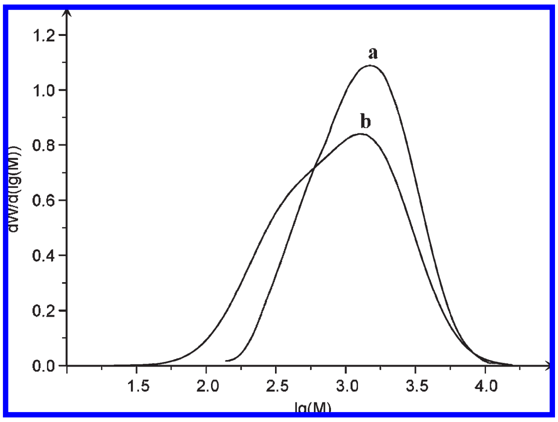

Figure 10. GPC curves for PEs prepared with L^{3Me} $Co^{II}Cl_2$, activated with MAO (a) and $AlMe_3$ (b) (runs 4 and 6 in Table 5).

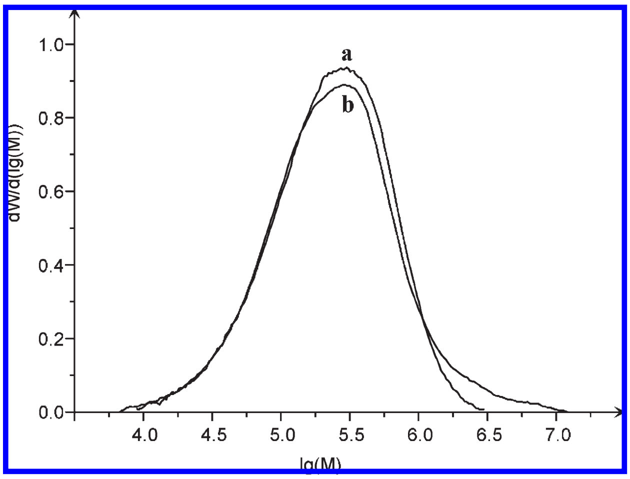

Figure 11. GPC curves for PEs prepared with $L^{tBu}Co^{II}Cl_2$, activated with MAO (a) and $AlMe_3$ (b) (runs 8 and 9 in Table 5).

The polymerization rate for the catalyst systems $L^{2Me}Co^{II}Cl_2$/MAO and $L^{2Me}Co^{II}Cl_2/AlMe_3$ was unstable. The C_p (active centers concentration) and k_p (propagation rate constant) values for polymerization over the system $L^{2Me}Co^{II}Cl_2$/MAO were determined.[48] It was found that the C_p value decreases by a factor of 1.6 (from 0.23 to 0.14 mol/mol(Co)) with the increase of the polymerization time from 5 to 15 min, whereas the values of the propagation rate constant (k_p) were almost independent on the reaction time. Analysis of the obtained data on the C_p and k_p values and the molecular mass characteristics of the resulted polymers drew the authors of ref 48 to conclude that the catalyst system $L^{2Me}Co^{II}Cl_2$/MAO contains only one type of active center and the reason for its deactivation with the increase of the polymerization time is the reduction of the number of active centers. Similar data on the catalyst behavior of $L^{2Me}Co^{II}Cl_2$ and $L^{3Me}Co^{II}Cl_2$ activated with MAO makes it possible to assume that similar active centers are formed in these catalyst systems.

Comparison of NMR and polymerization data obtained for the catalyst systems based on $LCo^{II}Cl_2$ ($L = L^{2iPr}$, L^{tBu}, L^{3Me}) can provide information about the active centers of these systems.

According to the assumption of Gibson et al.,[21] the only active species (or their immediate precursors) of the catalyst system $L^{2iPr}Co^{II}Cl_2$/MAO is the cobalt(I) ion pair $[L^{2iPr}Co^{I}(\eta\text{-}C_2H_4)]^+[\text{Me-MAO}]^-$. Our NMR studies show that at high [Al]/[Co] ratios (≥100) two types of cobalt species are present in the system $L^{iPr}Co^{II}Cl_2$/MAO: an ion pair of cobalt(II) (**2**) and an ion pair of cobalt(I) (**3**) (Scheme 2). However, in the presence of monomer, complex **2** rapidly converts into **3** ($[L^{2iPr}Co^{I}(S)]^+[\text{Me-MAO}]^-$), and, probably, only cobalt species of the type $\mathbf{3_{C2H4}}$ ($[L^{2iPr}Co^{I}(\eta\text{-}C_2H_4)]^+[\text{Me-MAO}]^-$) exist in the system $L^{2iPr}Co^{II}Cl_2/MAO/C_2H_4$ in conditions approaching real polymerization. This result is in agreement with the MWD data for the PE produced by the catalyst system $L^{2iPr}Co^{II}Cl_2$/MAO, which is typical for single-site catalysts ($M_w/M_n = 2.0$) (Table 5, run 1).

The polymerization activity of $L^{2iPr}Co^{II}Cl_2/AlMe_3$ and the resulting PE MWD value are very similar to that found for the $L^{2iPr}Co^{II}Cl_2$/MAO system (Table 5, run 2). As it was shown above, in the presence of ethylene, complexes of cobalt(I) of the type $[L^{2iPr}Co^{I}(\eta\text{-}C_2H_4)]^+[AlMe_3Cl]^-$ (**5**) were detected in the catalyst system $L^{2iPr}Co^{II}Cl_2/AlMe_3$. These complexes can be regarded as the immediate precursors of the polymerization active species formed in this system. Thus, the active species (or their precursors) of the $L^{2iPr}Co^{II}Cl_2$/MAO and $L^{2iPr}CoCl_2/AlMe_3$ systems are similar (ion pairs of cobalt(I), $\mathbf{3_{C2H4}}$ and **5**, respectively), differing only in the nature of counteranion. Polymerization activity of the catalyst system $L^{2iPr}Co^{II}Cl_2/AlMe_3/[CPh_3][B(C_6F_5)_4]$ was close to those of the $L^{2iPr}Co^{II}Cl_2$/MAO, and the obtained polymers were characterized by their identical GPC curves and MWD values (Table 5, runs 1 and 3). These results evidence that the nature of the counteranion has little effect on the catalyst properties of the cobalt complex. Hence, the initially different complexes of cobalt formed in the $L^{2iPr}Co^{II}Cl_2$/MAO and $L^{2iPr}Co^{II}Cl_2/AlMe_3$ systems convert upon interaction with ethylene into the similar active site precursors **3** ($\mathbf{3_{C2H4}}$) and **5**. This explains the close activities of the $L^{2iPr}Co^{II}Cl_2$/MAO and $L^{2iPr}Co^{II}Cl_2/AlMe_3$

---

(47) Semikolenova, N. V.; Zakharov, V. A.; Echevskaja, L. G.; Matsko, M. A.; Bryliakov, K. P.; Talsi, E. P. *Catal. Today* **2009**, *144*, 334–340.

(48) Barabanov, A. A.; Semikolenova, N. V.; Bukatov, G. D.; Matsko, M. A.; Zakharov, V. A. *J. Polym. Sci., Part B: Polym. Phys.* **2008**, *50*, 326–329.

systems and formation of the polymers with the same M_w and MWD values.

Polymerization activity of the catalyst systems based on $L^{3Me}Co^{II}Cl_2$ was noticeably higher than that of the systems obtained with complex $L^{2iPr}Co^{II}Cl_2$ (Table 5, runs 4–7). The PE samples obtained with $L^{3Me}Co^{II}Cl_2$ activated with MAO, MAO with a reduced content of $AlMe_3$ (MAO (20)), and $AlMe_3/[CPh_3][B(C_6F_5)_4]$ are characterized by low MW. Narrow MWD (M_w/M_n close to 2) of the studied polymers is characteristic for single-site catalysts. The MWD of the PE produced with the $L^{3Me}Co^{II}Cl_2/AlMe_3$ catalyst system was slightly broadened ($M_w/M_n = 2.6$, Table 5, run 6). Figure 10 shows the presence of a low molecular mass PE fraction, whereas the position of the peak, corresponding to the main polymer fraction, is close to that of the PE produced with MAO and $AlMe_3/[CPh_3][B(C_6F_5)_4]$ activators. Formation of the low molecular mass PE is not clear, and, possibly, it can be attributed to some fluctuations in the course of the polymerization run or more facile transmetalation in the case of TMA than MAO. Nevertheless, it is possible to conclude that upon activation of $L^{3Me}Co^{II}Cl_2$ with MAO and $AlMe_3$, similar cobalt(I) species $[L^{3Me}Co^{I}(\eta\text{-}C_2H_4)]^+[\text{Me-MAO}]^-$ (**8_{C2H4}**) and $[L^{3Me}Co^{I}(\eta\text{-}C_2H_4)]^+[AlMe_3Cl]^-$ (**10**) dominate in the reaction solution, determining formation of PE with close molecular structure.

$L^{tBu}Co^{II}Cl_2$/MAO and $L^{tBu}Co^{II}Cl_2/AlMe_3$ systems produce PE with noticeably higher MW ($M_w = (3.3-4.2) \times 10^5$, Table 5, runs 8 and 9) due to the presence of a bulky *t*-Bu substituent in the bis(imino)pyridyl ligand, hindering the chain transfer reactions. Figure 11 shows that the positions of a peak corresponding to the main polymer fraction of PEs produced with $L^{tBu}Co^{II}Cl_2$/MAO and $L^{tBu}Co^{II}Cl_2/AlMe_3$ are close. The moderate increase in the polydispersity value can be attributed to the formation of a small amount of high molecular mass PE. Both catalysts have close values of the initial activities and produce PE in similar yields. These data suggest that the close catalyst properties of the $L^{tBu}Co^{II}Cl_2$/MAO and $L^{tBu}Co^{II}Cl_2/AlMe_3$ systems are determined by close composition of the direct precursors of the active centers (cobalt(I) species denoted as **13** (**13_{C2H4}**) and **14** (Scheme 4)), as was shown above for the catalyst systems $LCo^{II}Cl_2$/MAO and $LCo^{II}Cl_2/AlMe_3$ ($L = L^{2iPr}$ and L^{3Me}).

In contrast to the catalysts described, the systems formed by activation of $L^{CF3}Co^{II}Cl_2$ with MAO and $AlMe_3$ proved to be highly active catalyst for ethylene oligomerization (Table 5, runs 10 and 11). These catalysts demonstrated high initial activity that drops with time more sharply than in the case of the catalyst systems based on $LCo^{II}Cl_2$ ($L = L^{2iPr}$, L^{tBu}, L^{3Me}) and after 10 min of polymerization were almost deactivated. This corresponds to the NMR data, showing that the intermediates formed in the $L^{CF3}Co^{II}Cl_2$/MAO ($AlMe_3$) system are less stable to degradation than those formed in the case of the $LCo^{II}Cl_2$/MAO ($L = L^{2iPr}$, L^{tBu}, L^{3Me}) analogues.

Conclusions

The cobalt(II) and cobalt(I) species, formed upon activation of $LCo^{II}Cl_2$ ($L = L^{3Me}$, L^{2iPr}, L^{tBu}, and L^{CF3}) with MAO, $AlMe_3/[CPh_3][B(C_6F_5)_4]$, and $AlMe_3$ were monitored by ^1H, ^2H, and ^{19}F NMR spectroscopy. It was shown that the ion pairs $[LCo^{II}(\mu\text{-Me})_2AlMe_2]^+[A]^-$, $[LCo^{II}Me(S)]^+[A]^-$, and $[LCo^{I}(S)]^+[A]^-$ can be observed in the catalyst systems $LCo^{II}Cl_2$/MAO and $LCo^{II}Cl_2/AlMe_3/[CPh_3][B(C_6F_5)_4]$ ($[A]^- = [\text{Me-MAO}]^-$ or $[B(C_6F_5)_4]^-$; S = toluene or vacancy), whereas neutral complexes $LCo^{I}(\mu\text{-Me})(\mu\text{-Cl})AlMe_2$ and $LCo^{I}(\mu\text{-Me})_2AlMe_2$ predominate in the catalyst systems $LCo^{II}Cl_2/AlMe_3$. Addition of monomer (C_2H_4) plays the key role in formation of the direct precursors of the polymerization active centers of the catalyst systems based on $LCo^{II}Cl_2$. In the case of the $LCo^{II}Cl_2$/MAO systems, addition of ethylene results in rapid reduction of cobalt(II) to cobalt(I), and only the ion pairs of the type $[LCo^{I}(S)]^+[A]^-$ are present in the reaction solution at 20 °C. In the case of the $LCo^{II}Cl_2/AlMe_3$ systems, in the presence of ethylene an ion pair with proposed structure $[LCo^{I}(\eta\text{-}C_2H_4)]^+[AlMe_3Cl]^-$ is the major cobalt species in the reaction solution. Similar intermediates (ion pairs of cobalt(I)) are present in the systems $LCo^{II}Cl_2/MAO/C_2H_4$ and $LCo^{II}Cl_2/AlMe_3/C_2H_4$. The results obtained can explain the close polymerization results (similar activity and PE structure) obtained with the catalyst systems based on $LCo^{II}Cl_2$ complexes activated with MAO and $AlMe_3$.

Experimental Section

General Experimental Details. Toluene was dried over molecular sieves (4 Å), purified by refluxing over sodium metal, and distilled under dry argon. Toluene-d_8 was dried over molecular sieves (4 Å), degassed in vacuo, and stored under dry argon. All experiments were carried out in sealed high-vacuum systems using break-seal techniques. $LCo^{II}Cl_2$ ($L = L^{3Me}$, L^{2iPr}, L^{tBu}, and L^{CF3})[6,20] were synthesized as described. Trimethylaluminum ($AlMe_3$) and $[CPh_3][B(C_6F_5)_4]$ were purchased from Aldrich. Methylaluminoxane (MAO) was obtained from Crompton GmbH (Bergkamen) as a toluene solution (total Al concentration 1.8 M, Al as $AlMe_3$ 0.5 M). For the purposes of this paper, MAO (or MAO(20)) with total Al content of 40 wt % and 10 mol % of Al as $AlMe_3$ was obtained as a solid product by solvent removal in vacuo at 20 °C from commercial MAO. ^1H and ^{19}F NMR spectra were recorded at 250.130 and 62.89 MHz, on a Bruker DPX-250 MHz NMR spectrometer. For the ^2H NMR spectra, a Bruker Avance-400 MHz NMR spectrometer was used. EPR spectra were measured on a Bruker ER-200D spectrometer at 9.3 GHz at room temperature.

NMR and EPR Sample Preparation. Sample preparation was carried out in sealed high-vacuum systems using break-seal techniques. Calculated quantities of the cobalt complexes were weighed, evacuated, and transferred into the NMR tube (length = 200 mm, *d* = 5 mm). Toluene-d_8, $AlMe_3$, or MAO (20) was added after $LCo^{II}Cl_2$ cooling in liquid nitrogen (77 K). In the case of $[CPh_3][B(C_6F_5)_4]$, this compound was transferred to the NMR tube (as a solution in the CH_2Cl_2 with subsequent solvent removal) before $LCo^{II}Cl_2$ addition.

Ethylene Polymerization Procedure. Polymerization was performed in a steel 1 L autoclave. Precatalysts (2.0×10^{-6} mol) were introduced into the autoclave in a vacuum-sealed glass ampule. The reactor was evacuated at 80 °C, cooled to 20 °C, and charged with the solution of a calculated cocatalyst amount in 150 cm^3 of toluene. After setting up the polymerization temperature (40 °C) and ethylene pressure (5 bar), the reaction was started by breaking the ampule of the complex. During the polymerization time (30 min), ethylene pressure, stirring speed, and temperature were maintained constant. The experimental unit was equipped with an automatic computer-controlled system for ethylene feed and recording of the ethylene consumption.

Polymer MW and MWD Measurements. Weight-average (M_w) and number-average (M_n) molecular weights and molecular weight distributions (M_w/M_n) were obtained by the GPC method with a Waters-150 at 150 °C with trichlorobenzene as a solvent.

Acknowledgment. This work was supported by the Russian Fund of Basic Research, Grant 09-03-00485.

The authors are grateful to A. V. Golovin for help with NMR spectroscopic studies. We are also grateful to L. G. Echevskaja and M. A. Matsko for help in the analysis of polymer MWD.

Supporting Information Available: NMR details for the complexes observed (J_{H-H} coupling constants, line half-widths). This material is available free of charge via the Internet at http://pubs.acs.org.